RSC Advances

ROYAL SOCIETY OF CHEMISTRY

www.rsc.org/advances

Cite this: DOI: 10.1039/c0xx00000x

www.rsc.org/Rscadvances

Paper

Novel quaternary phosphonium-type cationic polyacrylamide and elucidation of dual-functional antibacterial/antiviral activity

Yan Xue,[a] Yuanfeng Pan,[b] Huining Xiao[a]* and Yi Zhao[c]

A novel quaternary phosphonium-type cationic polyacrylamide which can kill bacteria via destroying cell membrane as well as inactivate adenovirus by blocking viral entry is developed.

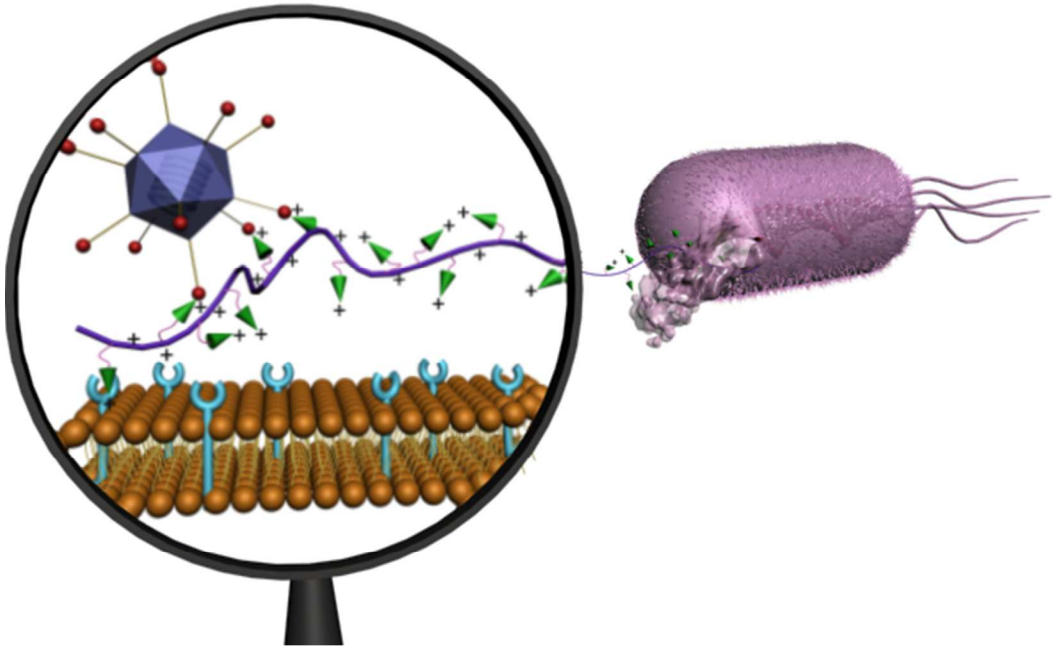

Cite this: DOI: 10.1039/c0xx00000x

www.rsc.org/rscadvances

PAPER

Novel quaternary phosphonium-type cationic polyacrylamide and elucidation of dual-functional antibacterial/antiviral activity

Yan Xue,[a] Yuanfeng Pan,[b] Huining Xiao[a]* and Yi Zhao[c]

Received (in XXX, XXX) Xth XXXXXXXXX 20XX, Accepted Xth XXXXXXXXX 20XX

DOI: 10.1039/b000000x

A novel quaternary phosphonium-type cationic polyacrylamide (PPAD) was developed with pendent butyltriphenylphosphonium bromide as the active moiety. A cationic monomer, diallyl dimethyl ammonium chloride (DADMAC), was introduced to impart positively charged groups to the backbone. The resulting cationic tripolymer was characterized with ^{13}C-^{1}H heteronuclear single quantum coherence (^{13}C-^{1}H HSQC), static light scattering (SLS), apparent charge density and UV spectrometry. The *in vitro* antibacterial activities of the synthesized polymers were investigated against *Escherichia coli* in terms of minimum inhibitory concentration (MIC). To investigate the antibacterial mechanism, atomic force microscopy (AFM) technique was employed for tracking the dynamic process of killing bacteria. The antiviral activity of copolymers was assessed via a plaque assay against non-enveloped adenovirus (ADV), and a model was established to reveal the mechanism of action of PPAD on adenovirus, correspondingly. Results indicated that the incorporation of quaternary phosphonium salt (QPS) can render cationic PAM antibacterial as well as antiviral activities, thus permitting the cationic tripolymer to be used as antibacterial/antiviral intensifier, retention or filtration aid for various hygiene products or water clarification/disinfecting process.

1. Introduction

The transmission and infection of pathogen, including microbe and virus, have resulted in serious threat for human being health and economic loss. With the increasing public health awareness, broad-active agents with long-term antimicrobial activity have aroused considerable interest. Compared with conventional low-molecular-weight biocides, chemically bonded polymeric agents have the advantages such as enhanced antimicrobial activity, efficiency and selectivity, reduced bacterial resistance and residual toxicity, prolonged stability and environmentally friendly performance. [1, 2] Covalent bonding of antimicrobial pharmacophores to polymer matrices would reduce or eliminate the permeation problems, which can be done either by polymerizing monomers with antimicrobial activity or by chemically anchoring antimicrobial moieties into the ordinary synthetic polymers.[3,4]

A number of studies have been performed on the antibacterial activity of low-molecular-weight and polymeric quaternary ammonium salts (QAS). However, due to the widespread use of QAS, the bacteria and fungi have developed resistance to such biocides, generating significantly weakened antimicrobial activity.[5,6] To address this problem, the novel alkyl quaternary phosphonium salts (QPS) with broad-spectrum and high efficient antimicrobial activity are being studied and applied. Research showed that the polymeric QPS exhibit a higher antimicrobial activity by two-orders of magnitude than the polymeric QAS with the same structure except the cationic part.[7,8] The fact is related to the intrinsical difference between P atom and N atom. The ionic radius of P atom is larger than that of N atom, which results in the stronger polarization effect, facilitating QPS to adsorb on the negatively charged bacteria more readily. [9] Furthermore, the molecular structure of QPS is relatively stable because of the weaker electronegativity of P atom. Therefore, QPS are inert to the common oxidizing and reducing agents, acids and bases. The features of QPS generate their wide application, which can be used in solutions with pH 2~12, while QAS can reach the optimum efficiency only at pH ≥ 9.0.[10] Kanazawa *et al.* studied a series of polymeric QPS as cationic biocides.[11] As the case of QAS, polymeric QPS were found to be much favored over the monomers in terms of adsorption onto the cytoplasmic membrane and the interaction with membrane followed by its disruption. Therefore, the antibacterial activity of the polymeric QPS is higher than that of the corresponding compounds. Kanazawa *et al.* prepared a series of polymeric QPS containing long alkyl chains (C_{10}-C_{18}) and studied their antibacterial performance against *Staphylococcus aureus* (*S. aureus*, Gram-positive) and *Escherichia coli* (*E. coli*, Gram-negative). It was found that the antibacterial activity of polymeric QPS decreased as the chain length increased due to the difficulty of diffusion through the cell wall for molecules with increasing molecular size. In terms of application, García-Argüelles *et al.* incorporated methyltriphenylphosphonium bromide into biodegradable polyesters for the preparation of antimicrobial wound dressings, and found QPS-containing polyesters showed significantly higher antimicrobial activity compared to that of QAS-containing polyesters. [12] Wu *et al.* intercalated QPS (tetradecyl tributyl

phosphonium bromide) into four clay minerals and the results demonstrated that the antimicrobial activity of clay minerals was promoted significantly after modification.[13] Gao *et al.* grafted polystyrene onto micron-sized silica gel and then covalently bounded QAS and QPS onto the PSt/SiO_2 particles, respectively.[14] The experimental results showed that both QAS-PSt/SiO_2 and QPS-PSt/SiO_2 possess strong antibacterial activity and QPS-PSt/SiO_2 has stronger antibacterial activity than the former one.

Besides the antibacterial activity, the antiviral activity of QPS has also been studied. Romanov *et al.* synthesized a series of QPS with different alkyl or aryl substitutes, and studied their ability to suppress the proliferation of influenza A virus (H3N2).[15] All of the investigated QPS compounds exhibited antiviral activity, and the activity exceeded the antiviral action of remantadine, a drug prescribed for the prevention and treatment of influenza A virus. By comparison, the two compounds propyltriphenyl-phosphonium bromide and butyltriphenyl-phosphonium bromide possess the highest chemotherapeutic index (CI 80,645), of which the toxicity for the chorion allantoid membrane was 250 ppm and the virucidal concentration for one viral dose was 0.0031 ppm. However, owing to the complexity of the synthesis process, there are few reports on the antiviral performance of polymeric QPS to date.

Polyacrylamide (PAM), a synthetic polymer with widespread applications in wastewater treatment, paper-making, enhanced oil recovery, soil conditioning, erosion control and medical appliances as well, has been the focus of a substantial amount of research since 1990s.[16] To render this polymer antimicrobial/antiviral is a current need of society, especially for the products used in the occasions that need a high degree of safety for the civilian population. As an additive for papermaking and wastewater treatment, PAM has been utilized as an intensifier, retention aid, filtration aid or flocculant according to its molecular weight.[17,18,19] In a number of paper products, such as tissue, paper towels, kitchen paper, food wrapper and bank notes, antimicrobial/antiviral agents are required to protect human beings from being attacked by bacteria or virus. Also in the process of water purification, disinfection and sterilization besides the removal of impurities are necessary.[20,21]

In this work we aimed at taking the advantage of QPS to impart antibacterial and antiviral properties to PAM further for paper products and water treatment. Due to the excellent antiviral activity and low cytotoxicity of butyltriphenylphosphonium bromide, its vinyl counterpart, (4-penten-1-yl)triphenylphosphonium bromide (PTPB), was chosen as the active comonomer. To further enhance the adsorption of PAM on fibers and the flocculation ability, one approach is to render PAM cationic groups, such as quaternary ammonium groups.[22,23] As a water-soluble cationic coagulant in water purification and retention agent in papermaking process, dially dimethyl ammonium chloride (DADMAC) was selected as the cationic component, which may act as a potential depressor of bacteria and fungi as well.[24,25] Herein, we reported the facile synthesis of a novel cationic PAM biocide/virucide (poly(PTPB-*r*-AM-*r*-DADMAC), PPAD) containing covalently bounded QPS via a free-radical solution polymerization. The antibacterial activities against *E. coli* and antiviral activities against adenovirus were investigated, and the mechanisms of action were elucidated, respectively. In addition to being bactericidal, the prepared cationic copolymer exhibited excellent virucidal activity at an extremely low dosage, *i.e.*, 100 ppm, close to its minimum inhibition concentration (MIC) against *E. coli*. The polymeric antimicrobial/antiviral agent eliminates the leaching problem encountered by traditional biocides; whereas the cationic groups providing positive charges facilitate the adsorption on fibers. The as-prepared cationic PAM is expected to be applicable in papermaking as wet-end functional additive to create value-added hygiene products, as well as in water purification as a dual-functional agent, *i.e.*, flocculant and disinfectant for water clarification and sterilization.

2. Experimental section

2.1 Materials

Acrylamide (AM), obtained from Sigma-Aldrich, was purified by recrystallization from acetone. (4-penten-1-yl)triphenylphosphonium bromide (PTPB), diallyldimethyl ammonium chloride (DADMAC, 65%), 2,2′-Azobis(2-methylpropionamidine) dihydrochloride (AIBA), deuterium oxide (D_2O), LB broth and phosphate buffered saline (PBS, one tablet pH 7.4) (all from Sigma-Aldrich), were used without further purification. Spectra/Pro cellulose dialysis membranes (molecular weight cut off, MWCO = 1,000 Da) were used to purify the products.

2.2 Test microorganisms

For the antibacterial assessment, colonies of gram-negative *E. coli* (ATCC 11229), provided by Canadian Research Institute for Food Safety (CRIFS) at the University of Guelph, were grown and maintained in nutrient broth prior to test. For the antiviral test, human embryonic kidney cell line (HEK 293), provided by IWK Health Centre at the Dalhousie University, grown in RPMI medium with 10% FBS (fetal bovine serum) was used. The non-enveloped stain utilized in the test was wild-type *adenovirus* (ADV), provided by IWK Health Centre at the Dalhousie University.

2.3 Characterizations

2.3.1 Nuclear Magnetic Resonance (NMR) Spectroscopy

The ^{1}H-NMR spectra were recorded in D_2O at 25ºC using an Oxford 300 spectrometer operating at 300.15 MHz. ^{13}C-NMR and ^{13}C-^{1}H heteronuclear single quantum coherence (^{13}C-^{1}H HSQC) spectra of tripolymer were obtained using an Oxford 400 spectrometer operating at 100.57 MHz for carbons and 399.94 MHz for protons in D_2O at room temperature.

2.3.2 Static light scattering (SLS)

The absolute weight-average M_ws of prepared polymers were determined via static light scattering. A 90PDP Brookhaven spectrophotometer equipped with a BI-APD avalanche photodiode was employed for the measurements at room temperature. A vertically polarized light of 656 nm wavelength from a diode laser was used as the incident beam. HPLC-grade toluene (refractive index = 1.4889, Rayleigh ratio = 1.137e-08) was used as the calibration liquid, and deionized water was used as the normalization solvent. The specific refractive index increments (*dn/dc*) of the polymer solutions were determined

using a BI-DNDC Brookhaven differential refractometer (λ_0 = 620 nm). The data analysis was conducted with a Brookhaven's 90Plus Debye plot analysis software.

2.3.3 Colloidal titration

The colloidal titration method conducted via Particle Charge Detector Mütek PCD 03 (Herrsching, Germany) was used to measure the apparent charge density of the cationic copolymer. 10 mL of dilute polymer solution with concentration of 0.05 g/L was titrated with the standard anionic polyelectrolyte (potassium polyvinyl sulfate (PVSK) solution) (concentration = 0.573 mM). The charge densities of the cationic polymers were calculated from the volume of the anionic polymer solution required to reach the end point over the titration. Three repeats were conducted to acquire an average value for each sample.

2.3.4 UV spectrophotometry

UV spectrum of the QPS monomer, PTPB, was recorded on an UV-Vis spectrophotometer (Genesys 10; Thermo Electron Corporation, Ohio, USA) using distilled water as the solvent. A calibration curve of absorbance *vs.* PTPB concentration was drawn at the wavelength where the maximum absorbance peak of PTPB was detected. The content of PTPB in cationic tripolymer could be determined according to the Beer-Lambert Law.

2.3.5 Atomic Force Microscopy (AFM)

AFM was used to investigate the antibacterial process of prepared polycations against *E. coli* at intervals. *E. coli* cells in LB broth were separated by centrifuging bacterial suspension (10^8 CFU/mL) at 5000 rpm for 1 min, and washed with sterile DD water twice and re-dispersed in DD water (10^7 CFU/mL, fresh *E. coli*). Treated *E. coli* suspensions were prepared by mingling fresh *E. coli* with PPAD solution (sample P6, 100 ppm) for 15 min and 30 min, respectively. Then the mixtures were centrifuged at 5000 rpm for 1 min, washed with sterile DD water twice and re-dispersed in DD water. Fresh and treated *E. coli* samples were dropped onto silicon plates (Universitywafer, South Boston) and dried in a fume hood. AFM imaging was performed with a Nanoscope IIIa (Veeco Instruments Inc., Santa Barbara, CA) in the tapping mode using etched silicon probes (NP-S20, Veeco Instruments) with a 0.3 Hz scan rate.

2.4 Copolymerization of PTPB and AM

To verify the feasibility of the copolymerization among PTPB, DADMAC and AM, the copolymerization of PTPB and AM was conducted firstly as follows: A 50 mL flask equipped with a magnetic stirring bar was charged with 0.41 g (1.0 mmol) of PTPB, 0.64 g (9.0 mmol) of AM and 20 mL of distilled water. The mixture was deoxygenated by purging with nitrogen for 30 min. Then the initiator AIBA (0.8 wt% of the total amount of the monomers) dissolved in 0.5 mL distilled water was added under a nitrogen atmosphere. The mixture was stirred for 10 h at 60°C. Afterwards, the solution was dialyzed against distilled water over 2 days and dried in vacuum to constant weight.

2.5 Synthesis of quaternary phosphonium tripolymer (PPAD)

The quaternary phosphonium tripolymers were synthesized via a free radical polymerization using AIBA as an initiator. A typical procedure of synthesis is described as follows: A 50 mL of round-bottom flask equipped with a magnetic stirring bar was charged with 20 mL of distilled water, 0.41 g (1.0 mmol) of PTPB, 0.50 g (7.0 mmol) of AM, and 30% of the total DADMAC aqueous solution (0.5 mL, 2.0 mmol). The mixture was deoxygenated by purging with nitrogen for 30 min. Then the initiator AIBA (0.8 wt% of the total amount of the monomers) dissolved in 0.5 mL distilled water was added via syringe. The reaction temperature was increased to 60°C. After an hour the remaining DADMAC solution was added dropwise and the mixture was stirred for 10 h at this temperature. Afterwards, the solution was dialyzed against distilled water over 3 days and dried in vacuum.

2.6 Antibacterial assessment

The minimum inhibition concentrations (MIC) of the synthesized copolymers with different QPS unit contents were determined following the standard procedures with slight modifications.[26] In general, fresh cultured colonies of *E. coli* were diluted with LB broth to an inoculum level of 10^6 CFU/mL. Two-fold serial solutions of the samples were prepared with sterile LB broth in glass tubes. The final concentrations of the polymer solution ranged from 500 to 1.75 ppm. Then, 0.2 ml of *E. coli* (10^6 CFU/mL) was added to the polymer/broth solutions, and seeded tubes were incubated at 37°C for 24 h. The MIC was interpreted as the lowest concentration that could inhibit the visible growth of bacteria compared with that of the control samples. Triple replica was used to obtain a mean value for each sample.

2.7 Antiviral assessment

The antiviral activity of prepared quaternary phosphonium tripolymer was evaluated via plaque assay on HEK 293 cells. Sample (P6) was tested at three concentrations of 25, 50 and 100 μg/mL (polymer was dissolved in phosphate buffer saline, PBS). The assay was performed as follows: 750,000 HEK 293 cells in 3 ml RPMI with 10% FBS were seeded per well using 6-well cell culture plates. The next day cell culture supernatant was removed and replaced with 2 mL media containing wild-type adenovirus with test polymer PBS solution. Cells were incubated for 2 h at 37°C with 5% CO_2. After incubation, cell culture supernatant was removed and 0.5% agarose in RPMI with 5% FBS was added. When agarose overlay had set, cells were incubated for 4 days and plaques were revealed using 0.03% neutral red solution. This stain can be only taken up by living cells instead of dead cells, resulting in only the living cells stained red. Each test was performed in triplicate.

The virucidal efficiency (%) was determined as follows:

$$\text{Virucidal efficiency (\%)} = (1-\frac{N}{M})\times 100\% \quad (1)$$

Where M and N are the numbers of the plaques detected from the control and treated samples, respectively.

3. Results and Discussion

3.1 Characterization of PPAD

The synthetic route of the quaternary phosphonium tripolymer is shown in Scheme 1. Copolymerization of PTPB, DADMAC and acrylamide was carried out via a free radical polymerization using AIBA as an initiator at 60°C for 10 h. Various monomer feed ratios were attempted to optimize the antimicrobial activity and

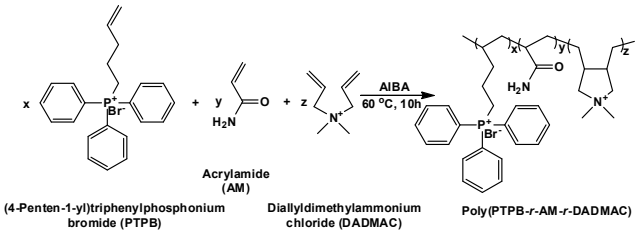

Scheme 1 Synthesis route of quaternary phosphonium tripolymer

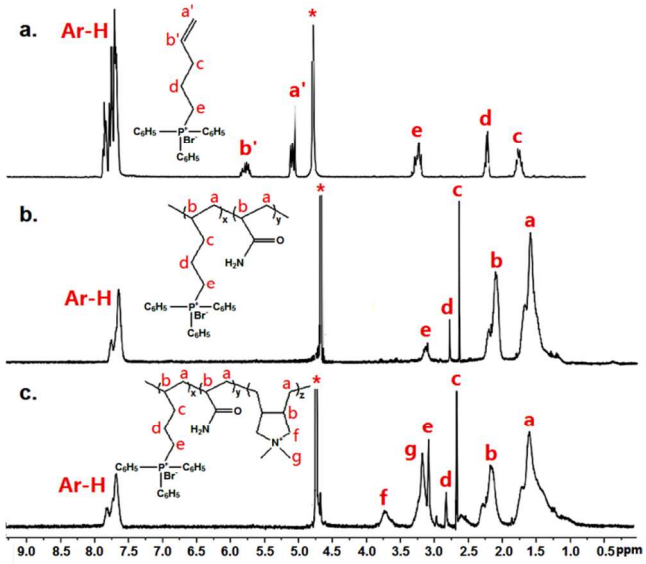

Fig. 1 ^{1}H-NMR spectra of (a) PTPB, (b) poly(PTPB-*r*-AM) and (c) poly(PTPB-*r*-AM-*r*-DADMAC) in D_2O. The signals originating from solvents are marked with asterisks.

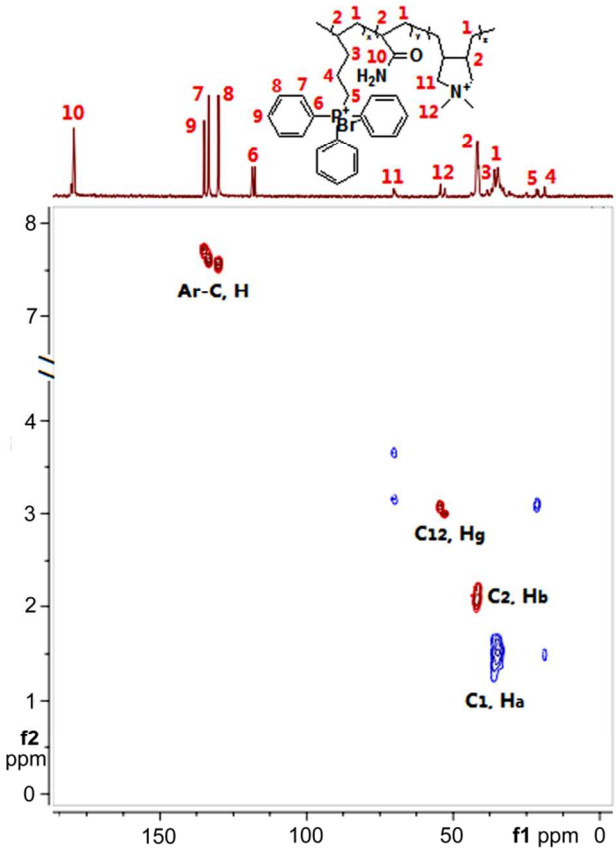

Fig. 2 ^{13}C-NMR and 2D NMR (^{13}C-^{1}H HSQC NMR) spectra of poly(PTPB-*r*-AM-*r*-DADMAC) in D_2O.

cationic charge density. To verify the feasibility of the reaction and the antimicrobial activity of PTPB polymer, the copolymerization was firstly conducted only using PTPB and acrylamide under the same reaction conditions. The molar feed ratio of PTPB to acrylamide was 10:90. ^{1}H-NMR spectrum of the synthesized copolymer is shown in Fig.1 (b). Fig.1 (a) is the spectrum of the monomer PTPB. By comparison, the vinyl proton signals at δ = 5.12 and 5.78 ppm disappeared, and the proton signals for methylene groups and methenyl groups appeared at δ = 1.18~1.78 and 2.02~2.36 ppm after copolymerization. Meanwhile, the signals for methylene groups of carbon chain on PTPB were also shifted from δ = 1.75 and 2.24 ppm to δ = 2.63 and 2.78 ppm, respectively. The ^{1}H-NMR spectra confirmed that the PTPB monomer could be copolymerized with acrylamide.

For antimicrobial and antiviral modification of PAM additives as wet-end functional additives for paper-making, PTPB and acrylamide could be further copolymerized with cationic monomer DADMAC at different feed ratios to tailor the cationic charge density. The copolymerization was carried out by dropwise adding the active monomer DADMAC into PTPB and acrylamide solution to obtain ideal compositions. The ^{1}H-NMR spectrum of poly(PTPB-*r*-AM-*r*-DADMAC) is assigned in Fig. 1(c). Compared with the spectrum of poly(PTPB-*r*-AM), new proton peaks appearing at δ = 3.22 and 3.73 ppm were assigned to the methyl and methylene protons of DADMAC.

Besides, ^{13}C-NMR and ^{13}C-^{1}H HSQC were also employed to confirm the structure of PPAD. As shown in Fig. 2, the attached ^{13}C-NMR spectrum presented a high intensity signal at δ = 179.36 ppm, which was attributed to the acylamino carbon C10. And the peak without coherence contours appeared at δ = 118.50 ppm, which was assigned to the phenyl carbon C6 directly attached to the phosphorus atom. In Fig. 2, the ^{13}C-^{1}H HSQC spectrum revealed the coherence between the chemical shifts of proton and carbon atoms. Two significant sets of cross-peaks appeared at δ = (34.46~36.94, 1.18~1.78) ppm and δ = (41.58~43.78, 2.02~2.36) ppm were attributed to the strong correlation between the carbons (C1, C2) and the directly attached protons in the backbone. The coherence contour groups appeared around δ = (134.9, 7.7) ppm were due to the correlation between the carbons and protons along the benzene ring.

To mitigate the intrusion into polymers and eliminate the absorption of cationic polymers onto the columns of GPC (Gel Permeation Chromatography) instrument, SLS measurement was carried out to determine the absolute M_w of prepared cationic polymers by constructing the Debye plot, from which the intercept yielded the inverse of the M_w and the slope yielded the second virial coefficient. The results are listed in Table 1, which shows the molecular weights of synthesized PPAD range from 30.6 to 33.4 kDa. In the as-prepared cationic tripolymer, PTPB

Table 1 Reaction parameter for the copolymerization of PTPB (M_1), AM (M_2) and DADMAC (M_3) and copolymer composition

Sample	Molar feed ratio ($M_1/M_2/M_3$)	PTPB unit content[a] (mol%)	DADMAC unit content[a] (mol%)	M_w[b] ($kg \cdot mol^{-1}$)
P1	10/90/0	9.8	0	32.5
P2	10/70/20	9.5	18.5	30.8
P3	15/70/15	10.2	16.2	33.4
P4	20/70/10	11.8	11.6	32.2
P5	20/50/30	12.1	28.3	31.5
P6	30/50/20	19.6	17.5	30.6
P7	40/50/10	22.8	11.4	33.2

a. Determined by ^{1}HNMR spectroscopy in D_2O.
b. Determined by SLS.

acted as the QPS antimicrobial/antiviral moiety, while DADMAC besides PTPB was incorporated as the cationic moiety. To determine the compositions of the tripolymers, the actual contents of PTPB and DADMAC units could be quantified via UV analysis and apparent charge density measurements. The UV-visible spectra of the monomer PTPB and poly(PTPB-*r*-AM-*r*-DADMAC) are shown in Fig. 3. In the spectrum of PTPB, the absorption peak at λ_{max} = 192 nm was assigned to the typical absorption of unconjugated alkene from aromatics. Compared with PTPB, the PPAD tripolymer presented a similar UV-vis spectrum. Because there was no phenyl group either in acrylamide or in DADMAC, the absorption peak at 192 nm might be attributed to the PTPB unit incorporated into the cationic copolymer. According to Beer-Lambert Law, the absorption intensity at 192 nm should increase with the increase of PTPB unit content in the polymer at the same polymer solution concentration. The actual content of PTPB unit in the copolymer was calculated consequently.

Based on the PTPB content and the result of charge density measurement, the DADMAC contents in the cationic tripolymers were calculated using the following formula:

$$\text{Actual DADMAC content (wt\%)} = M_{DAD} \times (\frac{cV}{m} - \frac{W_{PTPB}}{M_{PTPB}}) \times 100\% \quad (2)$$

Where

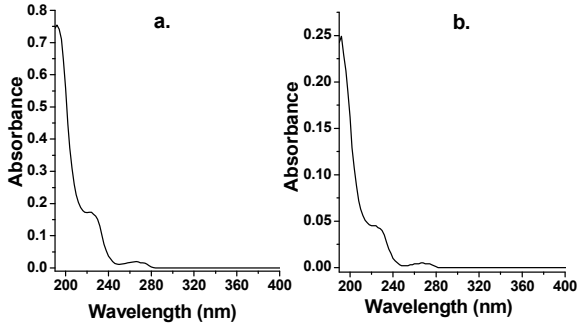

Fig. 3 UV-vis spectra of (a) PTPB (2.5 μg/mL in DD water), (b) poly(PTPB-r-AM- *r*-DADMAC) (sample P4, 2.5 μg/mL in DD water).

Table 2 Actual PTPB and DADMAC unit contents in the copolymers

Sample	PTPB unit content[a] (wt%)	PTPB unit content (mol%)	Charge density[b] (meq/g)	DADMAC unit content (mol%)
P1	35.6	8.7	0.87	0
P2	29.2	8.2	2.33	18.8
P3	34.5	10.1	2.19	16.2
P4	33.0	9.4	2.16	16.0
P5	34.2	10.9	2.79	25.8
P6	48.7	17.2	2.42	18.0
P7	55.3	20.4	2.15	12.1

a. Determined by UV spectrophotometer at 192 nm.
b. Determined by Particle Charge Detector Mütek PCD 03 using PVSK as the standard.

M_{DAD} = molar mass of DADMAC (g/mol)
c = concentration of standard anionic polyelectrolyte solution (mol/L)
V = volume of PVSK titrated to endpoint (L)
m = amount of cationic polymer (g)
W_{PTPB} = content of PTPB unit in the copolymer (wt%)
M_{PTPB} = molar mass of PTPB (g/mol)

The calculated results of PTPB unit contents in mass and molar percentage and DADMAC unit molar ratios converted from mass percentage are listed in Table 2. Both the actual contents of PTPB and DADMAC units in the copolymer, determined from UV analysis and charge density measurement, are close to the results determined from ^{1}H-NMR spectra, as listed in Table 1. Meanwhile, the actual contents of DADMAC units were comparable to the feed ratio, while that of PTPB units were lower than its feed ratio, especially for the polymers with high contents of PTPB units. Dropwise adding the active monomer during the copolymerization facilitated the incorporation of DADMAC into the copolymer. However, the steric hindrance of PTPB limited its copolymerization with AM and DADMAC in a large amount. In the copolymer sample with the highest feed ratio of PTPB (sample P7), the actual PTPB unit content was only 20.4 mol% which was lower than its desired value by 10.5%.

3.2 Antimicrobial assessment

Previous research indicated that QAS and QPS are more active against Gram-positive organisms than against Gram-negative bacteria.[27, 28, 29] The difference is attributed to the more complicated cell walls of Gram-negative bacteria, like *E. coli*, than Gram-positive bacteria, like *S. aureus*. The latter has a simple cell wall structure, in which there is only a rigid peptidoglycan layer outside the cytoplasmic membrane. The peptidoglycan layer, although relatively thick, is composed of networks with plenty of pores that cannot block foreign molecules into the cell. However, Gram-negative bacteria have another membrane outside the peptidoglycan layer, cephalin, of which the structure is similar to that of the cytoplasmic membrane.[30,31] The bilayer structure is a potential barrier against foreign molecules. Considering this, the antibacterial activity of prepared polymers against Gram-negative bacteria *E. coli* was tested in our study.

Fig. 4 shows the results of the *in vitro* antimicrobial activity of

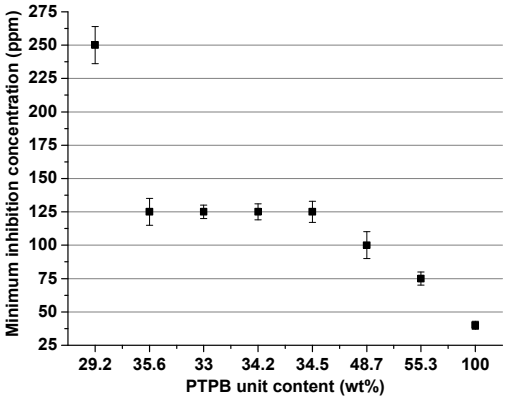

Fig. 4 Minimum inhibition concentration of PPAD against *E. coli* on the function of PTPB unit content.

PPAD as functions of PTPB contents. The quaternary phosphonium compound, PTPB, has a relatively low MIC value (around 40 ppm) against *E. coli*, indicating an effective antibacterial activity. With the increase of PTPB content in the tripolymer from 29.2 to 55.3 wt%, the MIC values of PPAD decreased from 250 to 75 ppm, indicating the enhanced antibacterial activities. Another matter worthy of note is that QAS is considered to possess antibacterial activity, and the activity is related to the length of the alkyl chain.[32] Previous study showed that the antibacterial activities of QAS compounds increase with the number of carbon atoms in the substituted alkyl chain.[33] DADMAC, a QAS which contains six carbon atoms in the alkyl chain, possesses a certain antimicrobial activity. However, in comparison with PTPB, DADMAC monomer has a much higher MIC value as 1000 ppm, suggesting that the antimicrobial activity of PPAD originated from the QPS instead of QAS.

The surface and morphological alterations of PPAD treated *E. coli* were revealed using AFM. Fig. 5 shows the amplitude images of fresh *E. coli* and PPAD treated *E. coli* at different contact times. A fresh *E. coli* is an elliptic shaped cell, of which the surface membrane looks compact and intact. As shown in Fig. 5 (A), the air dried *E. coli* can maintain the integrity of the cell, and no leaked residues were observed. After treated with 100 μg/mL of PPAD solution for 15 min, it can be seen from Fig. 5 (B) that the *E. coli* cell was shriveled to an irregularly condensed mass, of which the surface membrane collapsed, representing obvious grooves and indentations. Meanwhile, a small amount of leakage of cytoplasmic components was observed around the cell. After treated with PPAD for 30 min, *E. coli* cells were completely destructed and cleft into smaller fragments, resulting in indistinct individual bacterial cell as shown in Fig. 5 (C). It is postulated that the negatively charged surface of the bacterial cell is the target site of the polycations.[34] Therefore, the cationic PPAD firstly adsorbed onto the negatively charged lipopolysaccharide outer membrane of *E. coli* and initiated its penetration into cell. Consequentially, the membrane was disrupted, the permeability of the cell was increased and the periplasmic components were released followed by membrane slouging and bledding. With a time delay, the bacterial cells were completely disrupted, leaving only fragments of membranes.

From the dynamic records of AFM detecting the morphologic changes of treated *E. coli* cells, it is clear that the antibacterial mechanism of PPAD is to destroy the cell membranes, induce the leakage of the cytoplasmic components so as to deactivate the bacteria.

3.3 Virucidal assessment

Previous studies have demonstrated that polymeric QAS solutions and coatings, such as *N*-alkylated polyethylenimines (PEIs), have anti-influenza viral properties.[35,36,37] As a type of enveloped virus, influenza virus is protected by a lipid membrane. Therefore, the antiviral mechanism of aforementioned polycations is elucidated to penetrate the virus by disrupting the lipid envelope with the erect tentacles, thereby inactivating viruses. But for non-enveloped viruses, such as poliovirus, rotavirus and adenovirus, the foregoing mechanism does not apply.[38] Nonetheless, our study on the efficiency of PPAD solution in reducing the plaque formation of ADV virus indicated that polymeric QPS indeed possesses antiviral property against non-enveloped viruses.

As shown in Fig. 6, the PPAD sample with a MIC value against *E. coli* of 100 ppm also presented virucidal activity, which depended on the solution concentration. The virucidal efficiency of PPAD solution with a concentration of 100 ppm

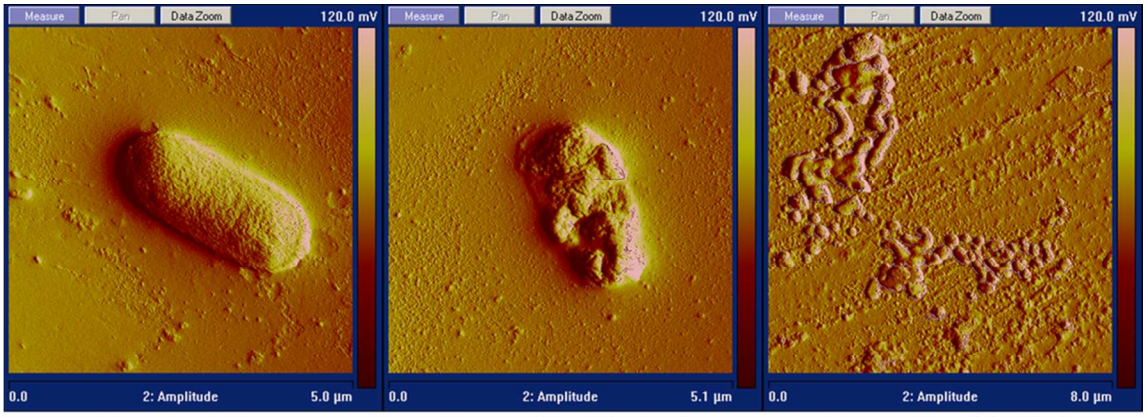

(A) Fresh E. Coli (B) Treated E. coli for 15 min (C) Treated E. coli for 30 min

Fig. 5 AFM images of *E. coli* cells treated with PPAD solutions for different intervals.

Cite this: DOI: 10.1039/c0xx00000x

www.rsc.org/rscadvances

PAPER

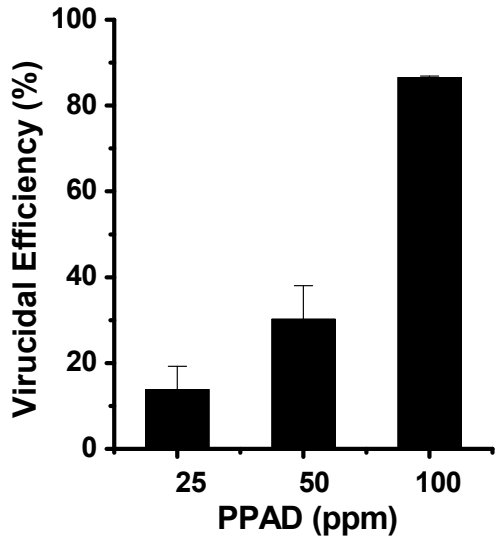

Fig. 6 Virucidal efficiency of PPAD against adenovirus.

reached up to 86.5%. To eliminate the possibility that the antiviral activity of PPAD might be induced by the cytotoxicity, its effect on the viability of uninfected HEK cells was evaluated using a neutral red stain. At concentrations of 25 ppm and 50 ppm, no toxic effect was induced. While at a higher concentration, *i.e.*, 100 ppm, some noticeable changes in the cellular morphology were observed, but cells remained viable.

Based on the test principle of plaque assay, it was assumed that the inhibition of viral infection caused by PPAD should be to interfere with the ability of viruses to infiltrate the target cells. That is caused either by damaging viral particles directly or by blocking the viral entry. For ADV viruses, belonging to a class of non-enveloped viruses, there are no lipid coats to be attacked by polycations. Furthermore, there is no evidence that polycations can destroy the protein capsids of viruses directly. Therefore, it was assumed that PPAD acted as an entry inhibitor through blocking the binding of non-enveloped viruses to the host cells. For both enveloped virus and non-enveloped virus, receptor binding is the essential first step in viral replication. Extensive studies have identified the coxsackie and adenovirus receptor (CAR) as the cellular receptor for adenoviral attachment and infection.[39,40,41] Adenovirus binding to CAR is initiated by the high affinity between the viral fibers, rod-shaped proteins protruding outward from the capsid vertices of ADV, and the cell surface CAR. The distal end of the fiber protein folds into a globular knob domain, possessing receptor-binding activity.[42,43] As revealed in Scheme 2(a1& a2), after the initial binding of the virus to the cell surface via the CAR-knob interaction, virus endocytosis occurs via the formation of clathrin-coated vesicles, accomplishing the virus entry. As a key component in receptor binding, the fiber knob has proven to be terminated with carboxyl groups. And a number of groups used this to modify ADV capsid, making ADV an efficient gene vector.[44,45,46,47] It is reasoned that ADV capsids can bind with polycationic molecules via noncovalent charge interaction due to the negative-charged fiber knob. As Scheme 2(b) illustrates, PPAD deactivates non-enveloped adenoviruses via the mechanism that PPAD interacts

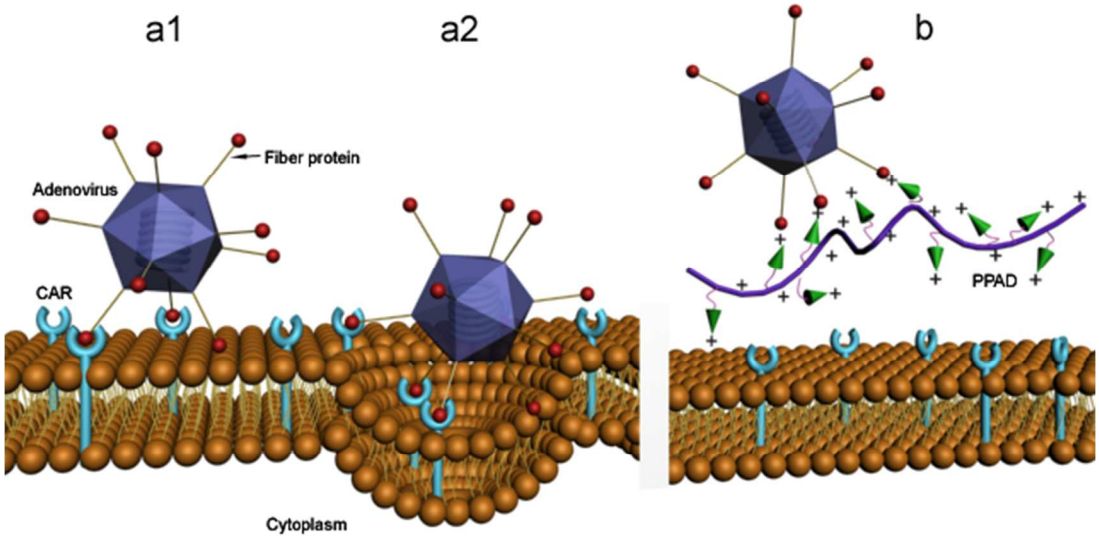

Scheme 2 A model for the role of PPAD in inhibiting ADV binding and entry into the host cell. (a1) Initial binding is mediated by the fiber protein of ADV that binds to the cell receptor, CAR; (a2) endocytosis is induced via the formation of clathrin-coated pit. (b) PPAD acts as an ADV entry inhibitor by blocking the ADV fiber protein from associating with the receptor.

with fiber knobs, consequently inhibiting the binding of virus with the cellular receptor CAR and blocking the cell entry.

4. Conclusions

Novel cationic PAM copolymers containing covalently bonded quaternary phosphonium salt were successfully synthesized with the controllable compositions. The antimicrobial activity of the resulting polymers were evaluated against *E. coli* and compared with that of PTPB and DADMAC monomers via MIC test. The incorporation of the antimicrobial moiety PTPB provides the copolymers with antimicrobial activity against Gram-negative bacteria with the lowest MIC at 75 ppm. The dynamic records of AFM demonstrated that following exposure to PPAD the bacterial cell membrane is destroyed, inducing the leakage of the cytoplasmic components so as to deactivate the bacteria. Plaque assay against adenovirus demonstrated that at a MIC concentration the PPAD sample exhibited a high virucidal efficiency of 86.5%. We propose that the negative-charged fiber knob of ADV might serve as binding sites for positive-charged PPAD, which inactivates ADV by blocking their cell entry. Therefore, the incorporation of PTPB can render cationic PAM not only antibacterial but also antiviral activity. The study described herein suggested that antimicrobial/antiviral cationic PAM could be a promising dual-functional additive for value-added paper products and water clarification and disinfection.

Acknowledgements

This study was financially supported by the NSERC strategic network SENTINEL-Bioactive Paper (Canada), and NSF China (No. 21306027 and No. 51379077). The authors would also like to thank Prof. T. Lin and Dr. A. MacNeil at the Dalhousie University for their help in the antiviral tests.

Notes and references

[a] *Department of Chemical Engineering, University of New Brunswick, Fredericton, NB, Canada. Fax: 506-453-3591; Tel: 506-453-3532; E-mail: hxiao@unb.ca*

[b] *School of Chemistry and Chemical Engineering, Guangxi University, Nanning, China*

[c] *School of Environmental Sci & Eng., North China Electric Power University, Baoding, China*

1 T. Ahamad, V. Kumar, S. Parveen and N. Nishat, *Appl. Organometal. Chem.*, 2007, **21**, 1013-1021.
2 M. Malmsten, *Soft Matter*, 2011, **7**, 8723-8736.
3 Y. Guan, H. Xiao, H. Sullivan and A. Zheng, *Carbohydrate Polymers*, 2007, **69**, 688-696.
4 Y. Chen, P. A. Wilbon, Y. P. Chen, J. Zhou, M. Nagarkatti, C. Wang, F. Chu, A. W. Decho and C. Tang, *RSC Adv.*, 2012, **2**, 10275-10282.
5 V. M. D'Costa, K. M. McGrann, D. W. Hughes and G. D. Wright, *Science*, 2006, **311**, 374-377.
6 S. Lu, G. Walters, R. Parg and J. R. Dutcher, *Soft Matter*, 2014, **10**, 1806-1815.
7 A. Kanazawa, T. Ikeda and T. Endo, *J. Polym. Sci., Part A: Polym. Chem.*, 1993, **31**, 335-343.
8 E. Kenawy, F. I. Abdel-Hay, A. E. R. El-Shanshoury, M. H. El-Newehy, *J. Control. Release.*, 1998, **50**, 145-152.
9 E. R. Kenawy and Y. A. G. Mahmoud, *Macromol. Biosci.*, 2003, **3**, 107-116.
10 R. Nudel, G. E. Janauer, E. E. Schrier and I. W. Figura, *US patent*, 1980, 4349646.
11 A. Kanazawa, T. Ikeda and T. Endo, *J. Polym. Sci., Part A: Polym. Chem.*,1993, **31**, 1441-1450.
12 S. García-Argüelles, Serrano, M. C. Gutiérrez, M. L. Ferrer, L. Yuste, F. Rojo and F. del Monte, *Langmuir*, 2013, **29**, 9525-9534.
13 T. Wu, A. G. Xie, S. Z. Tan and X. Cai, *Colloid. Surface. B: Biointerfaces*, 2011, **86**, 232-236.
14 B. Gao, Q. Liu and Y. Li, *J. Polym. Environ.*, 2010, **18**, 474-483.
15 G. V. Romanov, O. K. Pozdeev, G. K. Gilmanova, T. Y. Ryzhikova and E. P. Semkina, *Pharm. Chem. J.*, 1990, **24**, 414-417.
16 Y. Xue, Y. Guan, A. Zheng, H. Wang and H. Xiao, *J. Biomat. Sci. Polym. Ed.*, 2012, **23**, 1115-1128.
17 M. S. Khan, S. B. M. Haniffa, A. Slater and G. Garnier, *Colloid. Surface. Part B: Biointerfaces*, 2010, **79**, 88-96.
18 C. Ovenden and H. Xiao, *Colloid. Surf. A Physicochem. Eng. Asp.*, 2002, **197**, 225-234.
19 G. -Y. Kim, M. A. Hubbe and C. -H. Kim, *Ind. Eng. Chem. Res.*, 2010, **49**, 5644-5653.
20 Z. Jie, X. Yan, L. Zhao, S. D. Worley and J. Liang, *RSC Adv.*, 2014, **4**, 6048-6054.
21 K. S. Enger, K. L. Nelson, J. B. Rose and J. N. S. Eisenberg, *Water Res.*, 2013, **47**, 1181-1190.
22 M. Shirazi, T. G. M. van de Ven and G. Garnier, *Langmuir*, 2003, **19**, 10835-10842.
23 H. G. M. ven de Steeg, A. de Keizer, M. A. C. Stuart and B. H. Bijsterbosch, *Colloid. Surf. A: Physicochem. Eng. Asp.* 1993, **70**, 91-103.
24 N. K. Bhardwaj, T. D. Duong, V. Hoang and K. L. Nguyen, *J. Colloid. Interf. Sci.*, 2004, **274**, 543-549.
25 Y. Wang, J. Ni, C. Chen, J. Peng and H. Liu, J. Ind. Eng. Chem., 2014, DOI: 10.1016/j.jiec.2014.02.016.
26 Z. Ziaee, L. Qian, Y. Guan, P. Fatehi and H. Xiao, *J. Biomater. Sci. Polym. Ed.*, 2010, **21**, 1359-1370.
27 D. W. Blois and J. Swarbrick, *J. Pharm. Sci.*, 1972, **61**, 393-399.
28 A. Popa, C.M. Davidescu, R. Trif, G. Ilia, S. Iliescu and G. Dehelean, *React. Funct. Polym.*, 2003, **55**, 151-158.
29 N. Pasquier, H. Keul, E. Heine and M. Moeller, *Biomacromolecules*, 2007, **8**, 2874-2882.
30 K. Lienkamp, A. E. Madkour, A. Musante, C. F. Nelson, K. Nüsslein and G. N. Tew, *J. Am. Chem. Soc.*, 2008, **130**, 9836-9843.
31 E. Kenawy, F. I. Abdel-hay, A. E. R. El-shanshoury and M. H. El-newehy, *J. Polym. Sci.: Part A: Polym. Chem.*, 2002, **40**, 2384-2393.
32 F. Baudrion, A. Périchaud and E. Vacelet, *Biofouling*, 2000, **14**, 317-331.
33 G. Lu, D. Wu and R. Fu, *React. Funct. Polym.*, 2007, **67**, 355-366.
34 L. Qi, Z. Xu, X. Jiang, C. Hu and X. Zou, *Carbohydr. Res.*, 2004, **339**, 2693-2700.
35 J. Haldar, D. An, L. Álvarez de Cienfuegos, J. Chen and A. M. Klibanov, *PNAS.*, 2006, **103**, 17667-17671.
36 D. Botequim, J. Maia, M. M. F. Lino, L. M. F. Lopes, P. N. Simões, L. M. Ilharco and L. Ferreira, *Langmuir*, 2012, **28**, 7646-7656.
37 B. B. Hsu, S. Y. Wong, P. T. Hammond, J. Chen and A. M. Klibanov, *PNAS.*, 2011, **108**, 61-66.
38 G. McDonnell and A. D. Russell, *Clin. Microbiol. Rev.*, 1999, **12**, 147-179.
39 H. Matsui, F. Sakurai, K. Katayama, T. Yamaguchi, S. Okamoto, K. Takahira, M. Tachibana, S. Nakagawa and H. Mizuguchi, *Biomaterials*, 2012, **33**, 3743-3755.
40 M. Dimitrova, Y. Arntz, P. Lavalle, F. Meyer, M. Wolf, C. Schuster, Y. Haïkel, J. C. Voegel and J. Ogier, *Adv. Funct. Mater.*, 2007, **17**, 233-245.
41 X. Wang, Y. Deng, S. Li, G. Wang, E. Qin, X. Xu, R. Tang and C. Qin, *Adv. Healthc. Mater.*, 2012, **1**, 443-449.

42 M. R. Duffy, A. L. Parker, A. C. Bradshaw and A. H. Baker, *Nanomedicine*, 2012, **7**, 271-288.
43 Y. Zhang and J. M. Bergelson, *J. Virol.*, 2005, **79**, 12125-12131.
44 M. C. Bewley, K. Springer, Y. B. Zhang, P. Freimuth and J. M. Flanagan, *Science*, 1999, **286**, 1579-1583.
45 A. Vetter, K. S. Virdi, S. Espenlaub, W. Rödl, E. Wagner, P. S. Holm, C. Scheu, F. Kreppel, C. Spitzweg and M. Ogris, *Mol. Pharm.*, 2013, **10**, 606-618.
46 J. G. Smith, M. Silvestry, S. Lindert, W. Lu, G. R. Nemerow and P. L. Stewart, *PLoS Pathog.*, 2010, **6**, 1-11.
47 N. Tresilwised, P. Pithayanukul, P. S. Holm, U. Schillinger, C. Plank and O. Mykhaylyk, *Biomaterials*, 2012, **33**, 256-269.